Electronic Supplementary Material (ESI) for Journal of Materials Chemistry A.

Supporting information: The role of free volume, hydrogen bonds, and crosslinks on physical aging in polymers of intrinsic microporosity (PIMs)

Taigyu Joo,[a] Katherine Mizrahi Rodriguez,[b] Hyunhee Lee, [a] Durga Acharya,[c] Cara M. Doherty,[c] and Zachary P. Smith [a,*]

[a] Department of Chemical Engineering, Massachusetts Institute of Technology, Cambridge, MA 02139, United States

[b] Department of Materials Science and Engineering, Massachusetts Institute of Technology, Cambridge, MA 02139, United States

[c] The Commonwealth Scientific and Industrial Research Organization (CSIRO) Manufacturing, Private Bag 10, Clayton South 3169, Victoria, Australia

* Corresponding Author. Email address: zpsmith@mit.edu; Postal address: Massachusetts Institute of Technology, Department of Chemical Engineering, 77 Massachusetts Avenue, Room 66-466, Cambridge, MA, USA 02139-4307

Table of Contents

1. Chemical synthesis, film fabrication, and post-synthetic modifications

1.1. Materials

Methanol (≥99.9%), ethanol (pure, non-denatured), dichloromethane (DCM, ≥99.8%, stabilized with amylene), dimethylacetamide (DMAc, ≥99.8%, anhydrous), 1-methyl-2-pyrrolidinone (NMP, ≥99.5%, anhydrous), chloroform (≥99.9%, amylenes as stabilizer), toluene (≥99.8%, anhydrous), pyridine (≥99.9%), borane dimethyl sulfide complex solution (5.0 M in diethyl ether), hydrochloric acid (HCl, 37%), potassium carbonate (K_2CO_3, ≥99%), sodium hydroxide (NaOH, ≥98%, anhydrous pellets), and di-tert-butyl-dicarbonate (DTBDC, ≥99%) were purchased from *Millipore Sigma* and used as received without further purification. The PIM-1 monomers, 5,5',6,6'-tetrahydroxy-3,3,3',3'-tetramethyl-1,1'-spirobisindane (TTSBI, 96%) and tetrafluoroterepthalonitrile (TFTPN, 99%) were also purchased from *Millipore Sigma*, and they were purified using recrystallization and vacuum sublimation. H_2 (UHP300 99.999%), CH_4 (UHP300 99.99%), N_2 (UHP300 99.999%), and O_2 (UHP300 99.994%) were purchased from *Airgas*.

1.2. Monomer purification, PIM-1 synthesis, and film fabrication

TFTPN was purified using vacuum sublimation at 140–150 °C for approximately 2 h. TTSBI was purified by recrystallizing in methanol. To perform the recrystallization, 10 g of TTSBI was dissolved in 100 ml of methanol. The solution was concentrated by boiling until approximately half of the solution evaporated. After cooling the concentrated solution to approximately 40 °C, 20 ml of DCM was added and left to cool naturally in a chemical fume hood overnight. Fine white flakes that formed in the solution were vacuum filtered and dried in a vacuum oven at 60 °C overnight.

PIM-1 was synthesized via high-temperature step polymerization as previously reported,[1] but with slight modifications. TTSBI (5.106 g; 15 mmol), TFTPN (3.003 g; 15 mmol), and 30 ml of DMAc were stirred in a 3-neck round bottom flask at 300 rpm. After the monomers were completely dissolved, K_2CO_3 (6.210 g; 45 mmol) was added to the reaction flask, and the flask was submerged in a pre-heated oil bath at 160 °C. A Dean–Stark apparatus filled with toluene was attached to the flask, and a total of 25 ml of toluene was added to the reaction flask when the polymerization solution became too viscous to continue stirring. This addition of toluene was important to keep the reaction solution homogeneous, maintain solubility, and avoid crosslinking. After 60 min of the reaction, the flask was removed from the oil bath, and an additional 30 ml of toluene was added. The reaction solution was then poured slowly into methanol to precipitate the synthesized PIM-1. The precipitated PIM-1 was vacuum filtered and dried overnight at 130 °C. To purify PIM-1, it was dissolved again in 100 ml of chloroform and then reprecipitated in methanol. This purification step was repeated three times to remove residual solvent and low molecular weight polymerization products. Finally, the polymer was boiled in hot water for 5 h to remove salt, and it was dried in a vacuum oven at 130 °C overnight.

PIM-1 films were prepared using a standard solution-casting procedure. The PIM-1 polymer (0.1 g) was dissolved in 3.3 ml of chloroform (3 wt/v %) and stirred for 30 minutes. The solution was then filtered using a 0.45 μm syringe filter (*VWR, 76479-008*) into a 5 cm diameter STERIPLAN® glass Petri dish (*237554008, DWK Life Sciences*). The glass dish was covered with a piece of aluminum foil and a Petri dish cover to slow down the evaporation of chloroform. The solution was left inside a chemical fume hood for 72 h. The film was then detached from the Petri dish and dried in a vacuum oven at 130 °C for 12 h.

1.3. Post-synthetic modifications (PIM-NH_2 and PIM-NH_2-FVM)

PIM-NH_2 and PIM-NH_2-FVM films were synthesized using solid-state post-synthetic functionalization processes as previously reported.[2] In short, the cast PIM-1 films were submerged in excess 5.0 M borane dimethyl sulfide complex solution at 45 °C for 5 h. The resulting films were immersed in 1.0 M methanolic HCl for 8 h, and then the films were neutralized in a 5 wt% NaOH/DI water solution for 6 h. After the neutralization step, the films were repeatedly immersed and washed in DI water to remove NaOH from the films. The resulting PIM-NH_2 films were then dried in a vacuum oven at 130 °C for 12 h.

For PIM-tBOC, the PIM-NH_2 films were subsequently functionalized with tBOC groups by immersing approximately 0.3 g of the films in 40 ml of NMP, 686 µl of pyridine, and 2 ml of DTBDC at 35 °C for 24 h. The resulting PIM-tBOC films were washed with MeOH and DI water and then dried in a vacuum oven at 130 °C for 12 h. The dried PIM-tBOC films were treated in a vacuum oven at 250 °C for 27 h to thermally remove the tBOC groups to form PIM-NH_2-FVM. PIM-NH_2 films in this study were thermally annealed at 250 °C for 27 h to directly compare the effect of FVM with the non-protected analogues that experienced identical thermal processing. PIM-1 films only underwent the normal drying procedure at 130 °C for 12 h to serve as a benchmark polymer that has comparable drying conditions to other PIM-1 samples studied in the literature.

Table S1. Compiled density of PIM-1 using Archimedes' principle in literature.

Density	Solvent	Reference
1.21 ± 0.06	Water	This work
1.11	Water	2
1.18	Ethanol	9
1.1	Hexane	10
1.09	Hexane	11
1.112	-	12
1.1	Hexane	13
1.059	Ethanol	14
1.06	Ethanol	15
1.063	Ethanol	16
1.06	Alcohol	17
1.066	Fluorinert FC 77	18

Table S2. Compiled density of PIM-1 derivatives measured in our lab using Archimedes' principle.

Polymer	Density	Solvent	Note
PIM-1	1.21 ± 0.06	Water	This work
	1.11 ± 0.02	Water	
	1.22 ± 0.02	Water	
	1.18 ± 0.02	Heptane	
	1.14 ± 0.02	Decane	
	1.14 ± 0.01	Hexadecane	
PIM-NH_2	1.28 ± 0.02	Water	This work
	1.18 ± 0.02	Water	
	1.32 ± 0.02	Water	
	1.10 ± 0.02	Water	
	1.15 ± 0.01	Heptane	
	1.13 ± 0.01	Heptane	
	1.16 ± 0.01	Decane	
	1.15 ± 0.01	Hexadecane	
PIM-NH_2-FVM	1.25 ± 0.02	Water	This work
	1.15 ± 0.04	Water	

2. Pure-gas permeation experiments

Table S3. Kinetic diameter of gases considered in this work.

Gas	d (Å)
H_2	2.89
O_2	3.46
N_2	3.64
CH_4	3.80

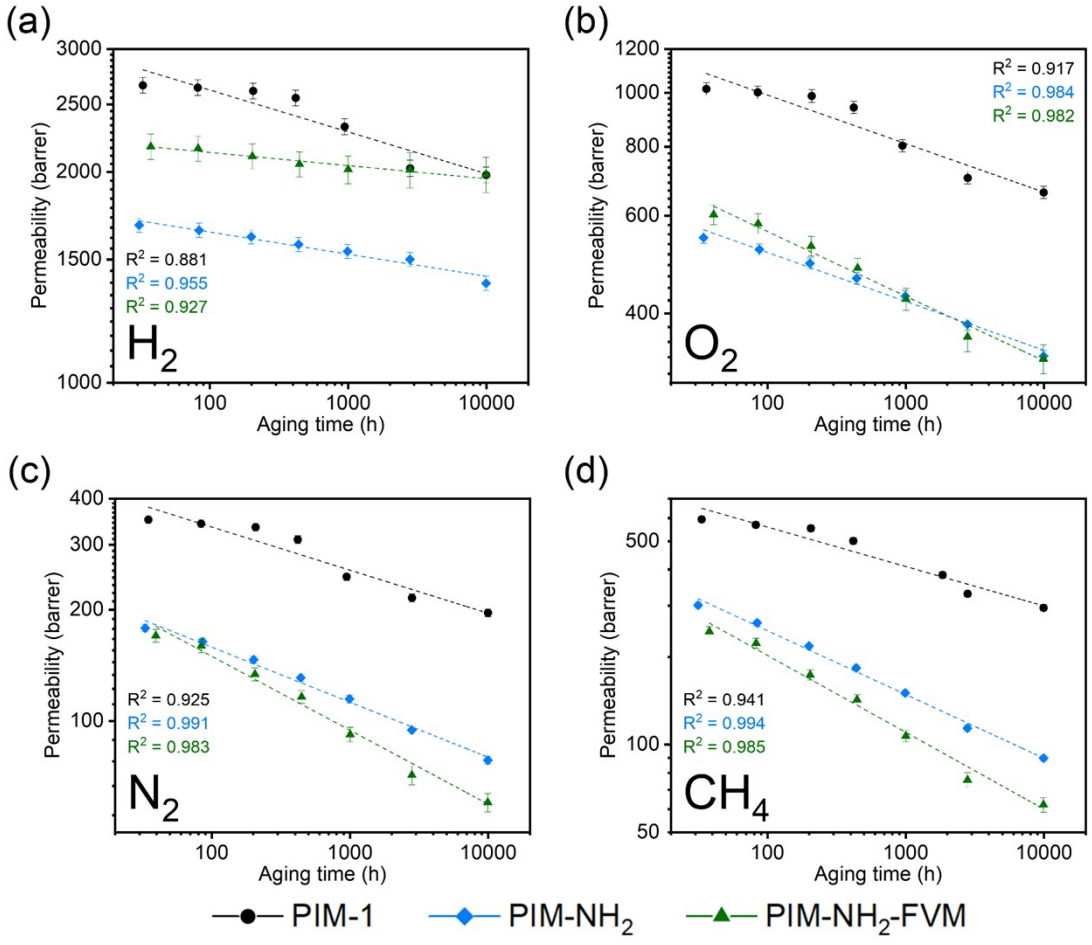

Figure S1. Comparison of aging behavior on an absolute scale by tracking pure-gas permeabilities of (a) H_2, (b) O_2, (c) N_2, and (d) CH_4 up to approximately 10,000 h. The linear fits of the experimental data on a log–log scale are shown in the dashed lines along with their R^2 values.

Table S4. Gas permeability and ideal selectivity of tested gases.

Polymer	Aging time[a] (h)	Permeability (barrer)				Selectivity	
		H_2	O_2	N_2	CH_4	H_2/CH_4	O_2/N_2
PIM-1	Fresh[b]	3380 ± 90	1250 ± 60	400 ± 30	590 ± 80	5.9 ± 0.8	3.1 ± 0.1
	33	2660 ± 70	1020 ± 30	350 ± 10	590 ± 10	4.5 ± 0.2	2.9 ± 0.1
	82	2640 ± 70	1000 ± 30	340 ± 10	570 ± 10	4.6 ± 0.2	2.9 ± 0.1
	206	2610 ± 70	990 ± 30	340 ± 10	550 ± 10	4.7 ± 0.2	2.9 ± 0.1
	419	2550 ± 70	940 ± 20	310 ± 10	500 ± 10	5.1 ± 0.2	3.0 ± 0.1
	948	2320 ± 60	800 ± 20	250 ± 10	380 ± 10[b]	6.1 ± 0.2	3.3 ± 0.1
	2824	2020 ± 50	700 ± 20	220 ± 10	330 ± 10	6.1 ± 0.2	3.3 ± 0.1
	10024	1980 ± 50	660 ± 20	200 ± 10	300 ± 10	6.7 ± 0.2	3.4 ± 0.1
PIM-NH_2	Fresh[b]	1450 ± 70	430 ± 10	134 ± 9	210 ± 20	6.8 ± 0.6	3.2 ± 0.1
	31	1680 ± 40	550 ± 10	180 ± 10	300 ± 10	5.6 ± 0.2	3.1 ± 0.1
	84	1650 ± 40	520 ± 10	160 ± 10	260 ± 10	6.3 ± 0.2	3.2 ± 0.1
	200	1610 ± 40	490 ± 10	150 ± 10	220 ± 10	7.4 ± 0.2	3.4 ± 0.1
	441	1570 ± 40	460 ± 10	130 ± 10	180 ± 10	8.6 ± 0.3	3.5 ± 0.1
	995	1540 ± 40	430 ± 10	110 ± 10	150 ± 10	10 ± 1	3.7 ± 0.1
	2815	1500 ± 40	380 ± 10	94 ± 2	110 ± 10	13 ± 1	4.0 ± 0.1
	10018	1390 ± 30	330 ± 10	78 ± 2	90 ± 2	16 ± 1	4.3 ± 0.1
PIM-NH_2-FVM	Fresh[b]	2000 ± 200	500 ± 100	120 ± 30	170 ± 50	13 ± 2	4.6 ± 0.5
	37	2170 ± 90	600 ± 30	170 ± 10	240 ± 10	8.9 ± 0.2	3.6 ± 0.2
	82	2160 ± 90	580 ± 20	160 ± 10	220 ± 10	9.7 ± 0.2	3.6 ± 0.2
	204	2110 ± 90	530 ± 20	130 ± 10	170 ± 10	12 ± 1	4.0 ± 0.2
	446	2050 ± 90	480 ± 20	120 ± 10	140 ± 10	14 ± 1	4.2 ± 0.2
	1006	2020 ± 90	420 ± 20	92 ± 4	110 ± 10	19 ± 1	4.6 ± 0.3
	2819	2010 ± 120	360 ± 20	71 ± 4	75 ± 4	27 ± 1	5.1 ± 0.4
	9998	1980 ± 120	330 ± 20	60 ± 3	62 ± 4	32 ± 3	5.5 ± 0.5

The errors are calculated from propagation of uncertainty.

[a]The presented time is the aging time at the start of hydrogen permeation test. All tests were completed within 6 hours unless indicated otherwise.

[b]Permeability and selectivity of polymer samples from the previous study[2] are included for comparison.

[c]Methane was retested for this point at a later time (aging time = 1,859 h).

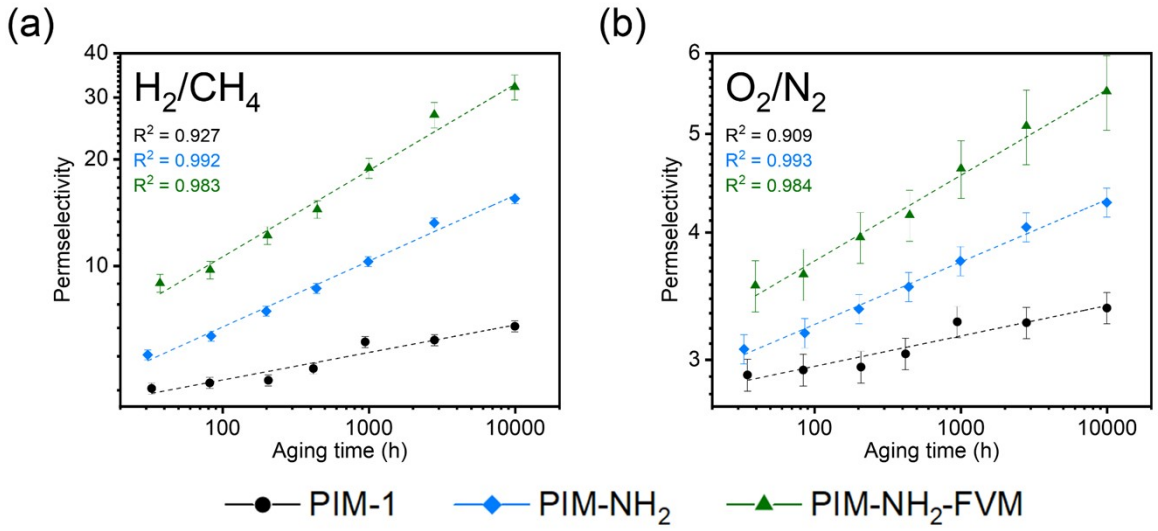

Figure S2. Comparison of selectivity as a function of time up to 10,000 h on an absolute scale for (a) H_2/CH_4 and (b) O_2/N_2. The linear fits of the experimental data on a log–log scale are shown in the dashed lines along with their R^2 values.

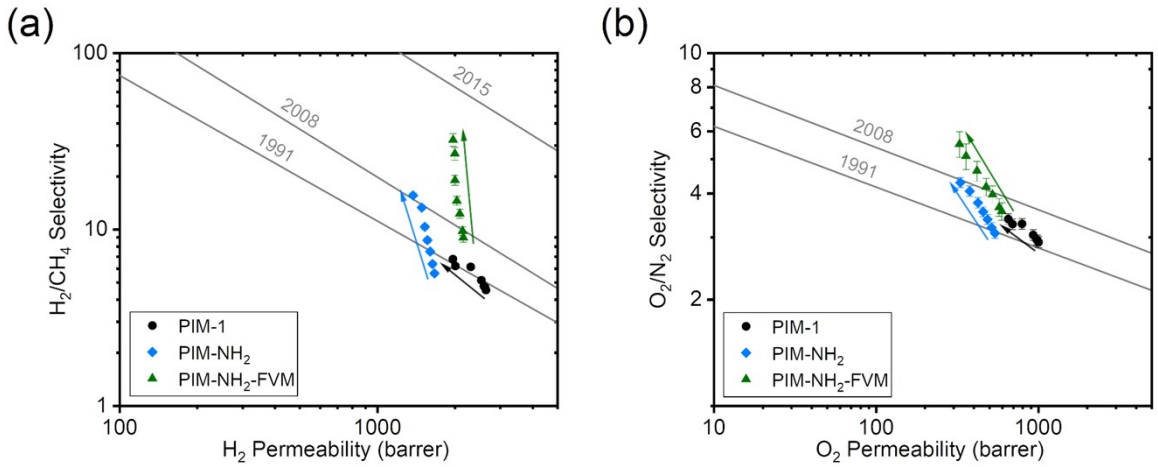

Figure S3. Comparison of aging behavior presented in (a) H_2/CH_4 and (b) O_2/N_2 upper bound plots.

Table S5. A summary of permeability aging rate constants (β_P) extracted from aging curves for H_2, O_2, N_2, and CH_4.

Polymer	Gas	β_P
PIM-1	H_2	0.060
	O_2	0.086
	N_2	0.117
	CH_4	0.135
PIM-NH_2	H_2	0.032
	O_2	0.088
	N_2	0.149
	CH_4	0.219
PIM-NH_2-FVM	H_2	0.018
	O_2	0.118
	N_2	0.203
	CH_4	0.266

Table S6. A summary of slopes obtained from linear fits of aging rate constants (β_P) in a semi-long scale, highlighting the influence of penetrant size on physical aging behavior.

Polymer	Slope	Ref
PIM-NH_2	0.137	This work
PIM-NH_2-FVM	0.199	This work
PIM-1	0.058	This work
	0.062	3
	0.098	4
	0.057	5
	0.039	6
	0.089	7
	0.091	8

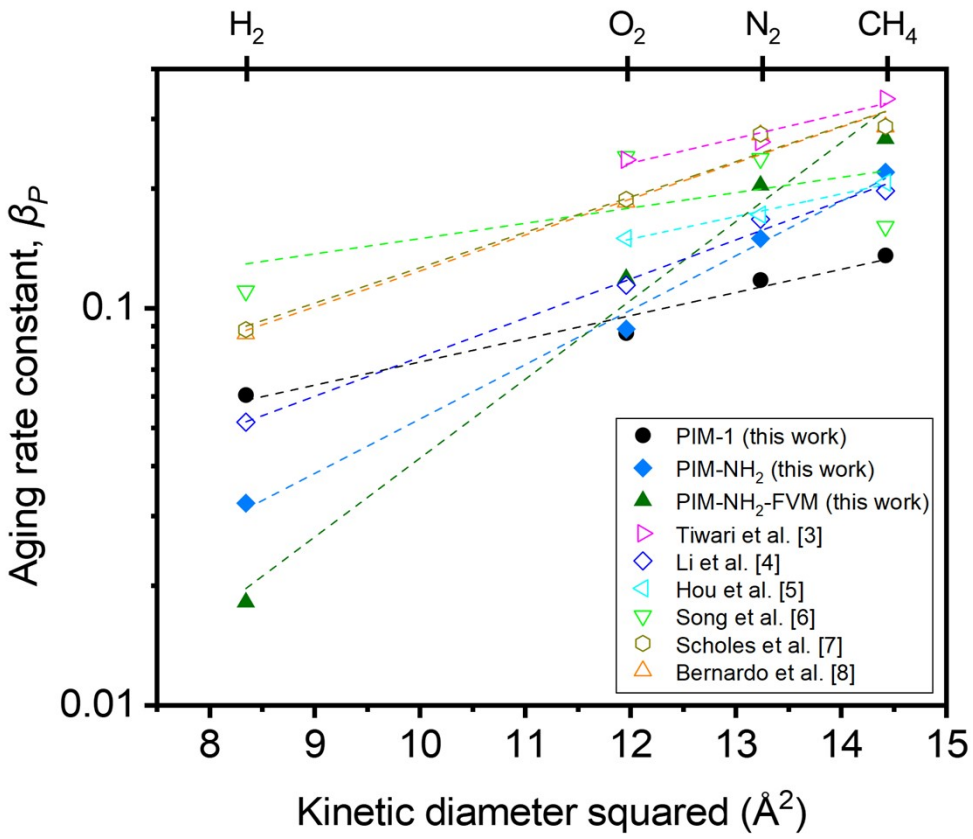

Figure S4. Permeability aging rate constants (β_P) of PIM-1 extracted from aging curves in literature for H_2, O_2, N_2, and CH_4.[3–8] The dashed lines are linear fits of β_P on a semi-log scale.

3. Pure-gas permeation experiment - reproducibility test

Table S7. A summary of information on the replicate samples, including the number of samples tested, thickness, density, fractional free volume (FFV) calculated from the group contribution method, drying conditions, and post-treatment conditions. All uncertainties are noted as standard deviations.

Polymer	PIM-1	PIM-NH_2	PIM-NH_2-FVM
Number of samples	3	4	3
Thickness (μm)	40.6 ± 3.6	46.0 ± 8.0	55.9 ± 9.1
Density (g/cm^3)	1.21 ± 0.06	1.28 ± 0.02	1.25 ± 0.02
FFV_{group}[a]	0.23 ± 0.04	0.16 ± 0.01	0.18 ± 0.01
Drying conditions	Vacuum, 130 °C, 12 h	Vacuum, 130 °C, 12 h	Vacuum, 130 °C, 12 h
Post-treatment conditions	n/a	Vacuum, 250 °C, 27 h	Vacuum, 250 °C, 27 h

[a]Light urea crosslinks were not considered in the calculation.

Table S8. Gas permeability and ideal selectivity of tested gases for the replicate samples. All uncertainties are noted as standard deviations.

Polymer	Aging time[a] (h)	Average permeability (barrer)				Average selectivity	
		H_2	O_2	N_2	CH_4	H_2/CH_4	O_2/N_2
PIM-1	32 ± 2	3350 ± 530	1160 ± 190	350 ± 70	520 ± 130	6.9 ± 2.3	3.3 ± 0.4
	81 ± 2	3310 ± 510	1140 ± 170	340 ± 60	500 ± 120	7.1 ± 2.3	3.4 ± 0.4
	207 ± 1	3260 ± 490	1130 ± 140	340 ± 40	500 ± 90	6.8 ± 1.8	3.4 ± 0.3
	427 ± 10	3170 ± 480	1080 ± 140	320 ± 30	460 ± 70	7.0 ± 1.5	3.4 ± 0.3
	962 ± 21	2900 ± 470	870 ± 90	230 ± 20	320 ± 50[b]	9.4 ± 2.4	3.8 ± 0.4
PIM-NH_2	31 ± 1	2360 ± 500	760 ± 170	240 ± 50	360 ± 70	6.5 ± 0.7	3.2 ± 0.1
	87 ± 7	2300 ± 500	710 ± 160	220 ± 50	320 ± 70	7.3 ± 0.9	3.3 ± 0.1
	213 ± 11	2260 ± 520	680 ± 170	200 ± 60	270 ± 80	8.4 ± 1.2	3.5 ± 0.2
	428 ± 8	2230 ± 540	650 ± 180	180 ± 50	240 ± 80	9.4 ± 1.3	3.6 ± 0.1
	1004 ± 15	2170 ± 530	610 ± 170	170 ± 50	220 ± 70	10 ± 1	3.7 ± 0.1
PIM-NH_2-FVM	35 ± 2	3110 ± 880	840 ± 270	220 ± 80	300 ± 120	11 ± 3	3.8 ± 0.3
	81 ± 1	3040 ± 890	780 ± 290	200 ± 90	260 ± 130	13 ± 5	4.0 ± 0.5
	423 ± 19	2950 ± 850	670 ± 290	160 ± 80	190 ± 110	20 ± 9	4.6 ± 0.7
	1007 ± 8	2810 ± 740	590 ± 260	130 ± 70	130 ± 70	24 ± 11	4.8 ± 0.7

The error bars indicate standard deviations.

[a]The presented time is the aging time at the start of hydrogen permeation test. All tests were completed within 6 hours unless indicated otherwise.

[b]Methane was retested for this point for one sample at a later time (aging time = 1,267 ± 420 h).

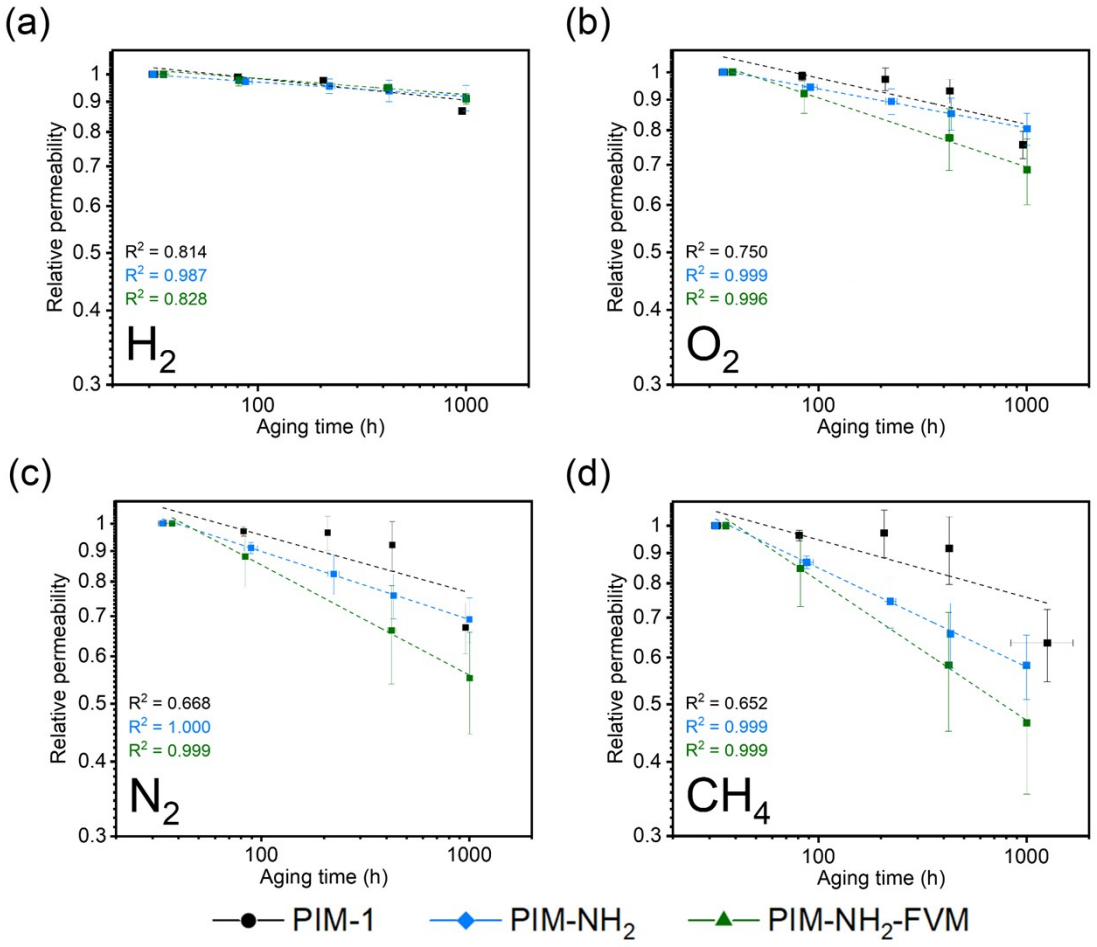

Figure S5. Comparison of (a) H_2, (b) O_2, (c) N_2, and (d) CH_4 aging behavior on a normalized scale for the replicate samples. The linear fits of the experimental data on a log–log scale are shown in the dashed lines along with their R^2 values.

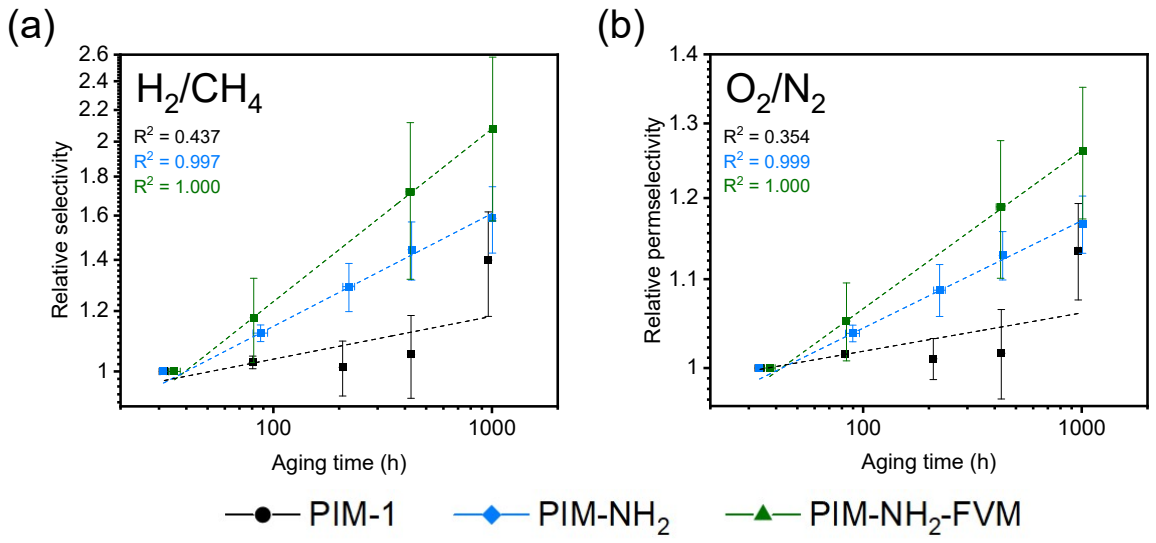

Figure S6. Comparison of (a) H_2/CH_4 and (b) O_2/N_2 permselectivity as a function of time on a normalized scale for the replicate samples. The linear fits of the experimental data on a log–log scale are shown in the dashed lines along with their R^2 values.

4. Pure-gas sorption experiments

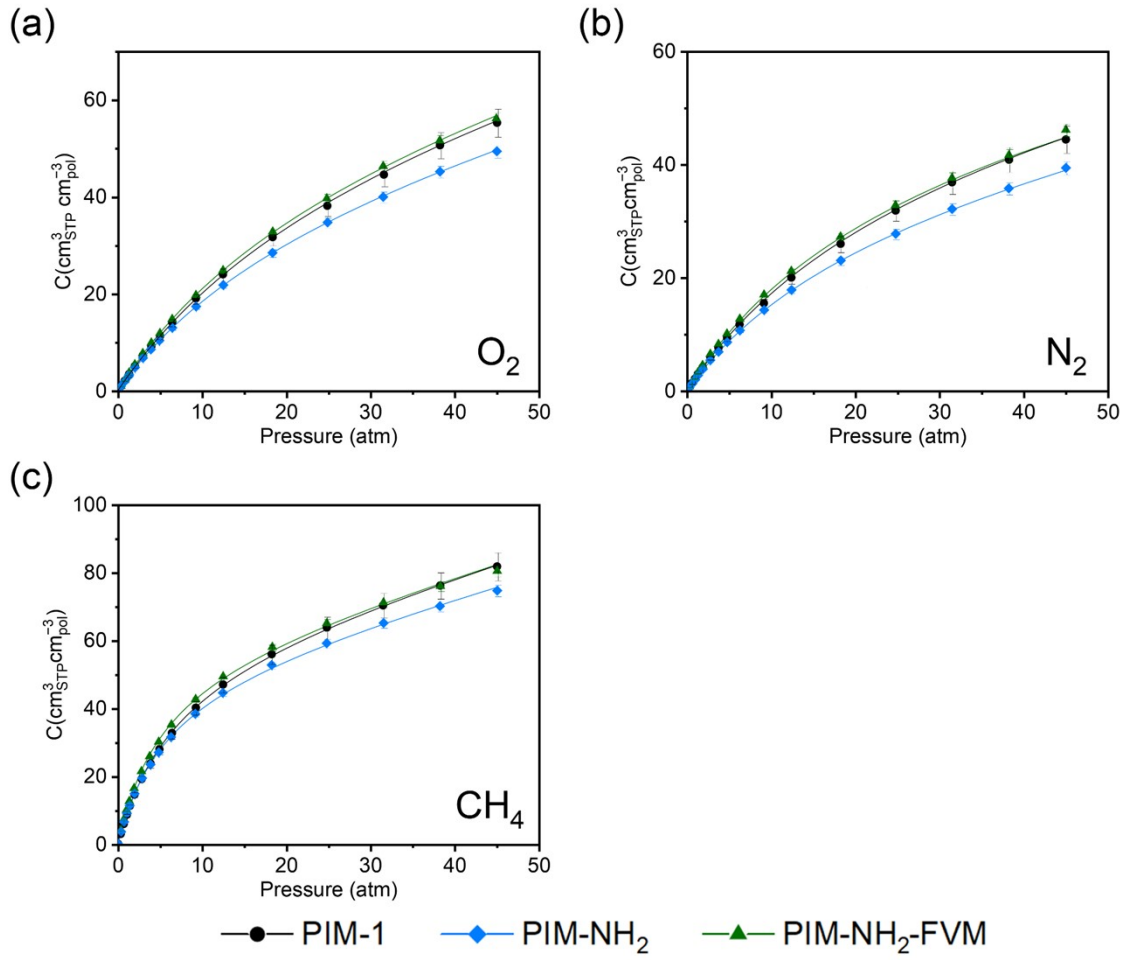

Figure S7. Sorption isotherms comparison and dual-mode sorption fittings for (a) O_2, (b) N_2, and (c) CH_4 for fresh films of PIM-1, PIM-NH_2, and PIM-NH_2-FVM measured at 35 °C.

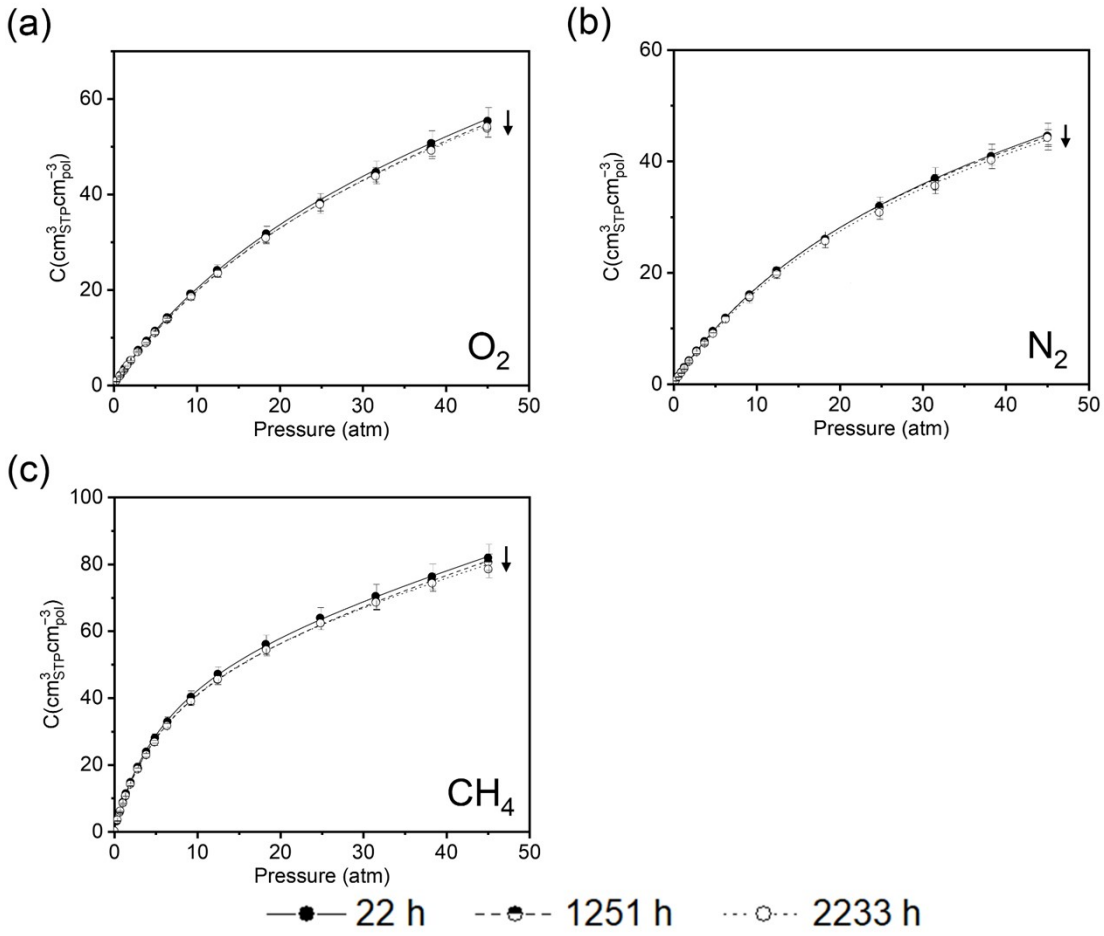

Figure S8. Sorption isotherm comparison and dual-mode sorption fittings for (a) O_2, (b) N_2, and (c) CH_4 for PIM-1 at three different aging times measured at 35 °C.

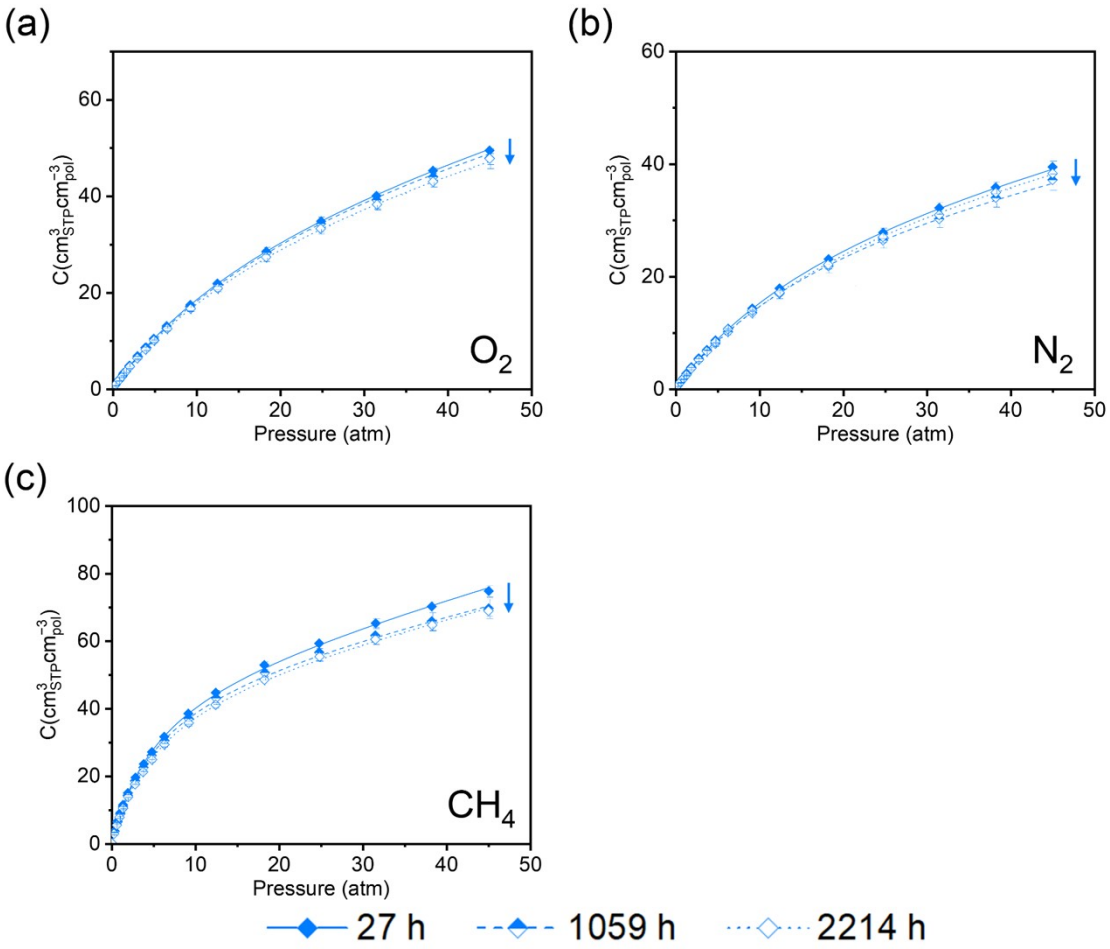

Figure S9. Sorption isotherm comparison and dual-mode sorption fittings for (a) O_2, (b) N_2, and (c) CH_4 for PIM-NH_2 at three different aging time measured at 35 °C.

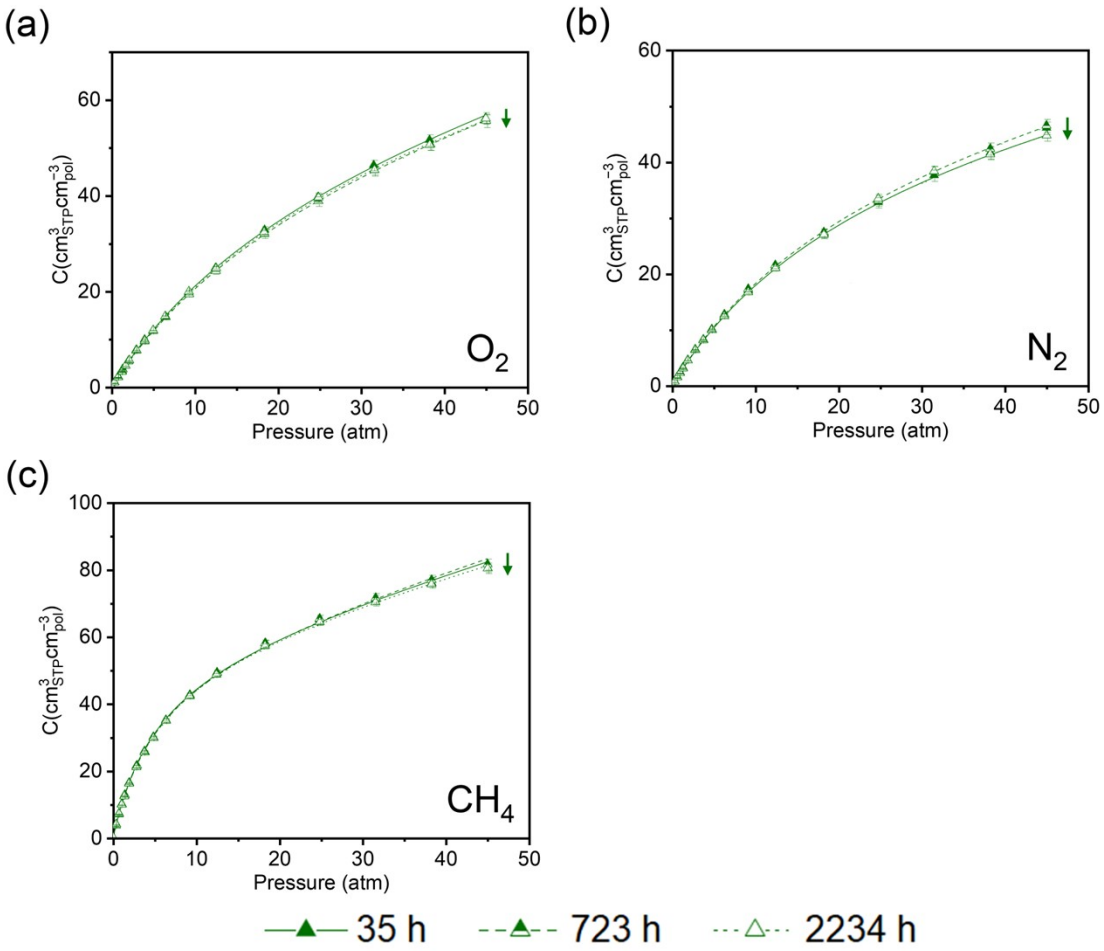

Figure S10. Sorption isotherm comparison and dual-mode sorption fittings for (a) O_2, (b) N_2, and (c) CH_4 for PIM-NH_2-FVM at three different aging time measured at 35 °C.

Table S9. Dual-mode sorption (DMS) model parameters fitted to experimental data.

Polymer	Gas	PIM-1			PIM-NH_2			PIM-NH_2-FVM		
		22 h	1251 h	2233 h	27 h	1059 h	2214 h	35 h	723 h	2234 h
k_D ($cm^3_{STP}\, cm^{-3}_{pol}\, atm^{-1}$)	O_2	0.39	0.37	0.35	0.41	0.34	0.35	0.44	0.43	0.36
	N_2	0.25	0.21	0.21	0.28	0.23	0.24	0.30	0.28	0.22
	CH_4	0.70	0.73	0.67	0.65	0.54	0.57	0.70	0.74	0.66
C_H' ($cm^3_{STP}\, cm^{-3}_{pol}$)	O_2	62.3	63.7	63.7	47.3	52.9	48.7	57.0	56.4	63.3
	N_2	53.1	55.8	56.1	39.1	38.7	42.4	46.7	51.2	53.8
	CH_4	58.1	55.0	57.1	52.2	51.8	49.7	56.8	55.9	57.8
b (atm^{-1})	O_2	0.035	0.033	0.034	0.043	0.038	0.040	0.041	0.040	0.037
	N_2	0.038	0.037	0.035	0.046	0.046	0.040	0.048	0.043	0.041
	CH_4	0.151	0.153	0.148	0.177	0.174	0.169	0.190	0.188	0.182

The presented time is the aging time at the start of oxygen sorption test.

5. Effective diffusivity and sorption coefficient data

Table S10. Diffusion coefficients and sorption coefficients of H_2, O_2, N_2, and CH_4 for the polymers studied in this work.

Polymer	Aging time[a] (h)	Diffusion coefficient[b] ($10^{-7} cm^2\ s^{-1}$)			Sorption coefficient[c] ($cm^3_{STP}\ cm^{-3}_{pol}\ atm^{-1}$)		
		O_2	N_2	CH_4	O_2	N_2	CH_4
PIM-1	22	29.4	12.0	5.94	2.50	2.18	8.29
	2233	23.6	8.41	3.48	2.42	2.10	8.01
PIM-NH_2	27	16.2	6.09	2.66	2.36	2.01	8.50
	2314	13.2	3.99	1.21	2.23	1.88	7.75
PIM-NH_2-FVM	35	15.3	4.72	1.90	2.69	2.42	9.76
	2234	11.1	2.56	0.70	2.64	2.35	9.52

[a]The presented time is the aging time at the start of oxygen sorption test.
[b]Permeabilities at corresponding sorption test times were calculated from the linear fits of the experimental data in log–log scale, shown in **Figure 2**. The diffusion coefficients were then calculated using the sorption–diffusion model.
[c]The sorption coefficients were calculated using the dual-mode sorption model, using the fitting parameters in **Table S9** and the testing pressure of 15 psia.

6. Variable-temperature permeation experiments

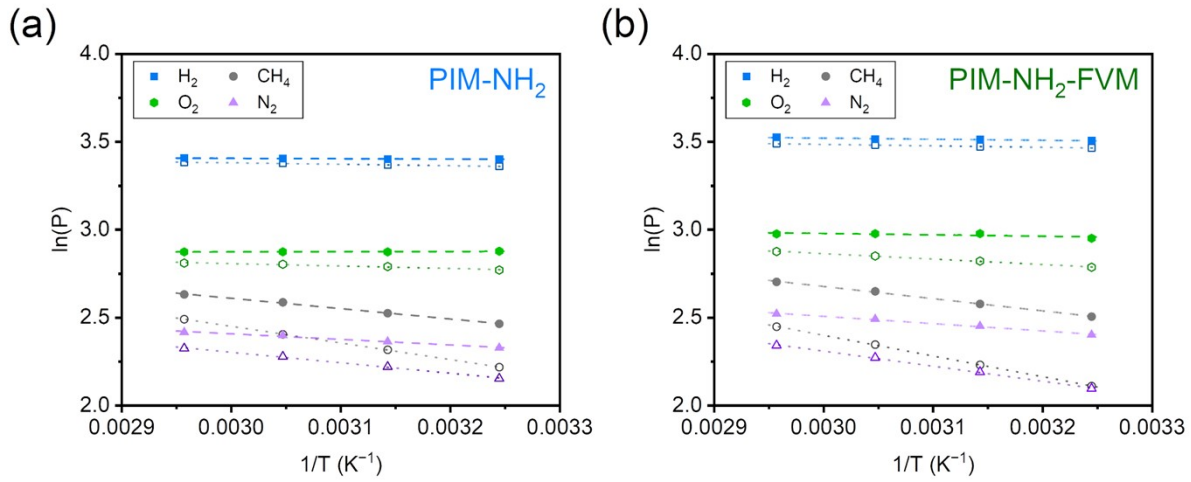

Figure S11. Comparison of Arrhenius plots for fresh and aged (a) PIM-NH_2 and (b) PIM-NH_2-FVM membrane films. The lighter and filled symbols indicate fresh samples and the darker and unfilled symbols indicate aged samples (710 h).

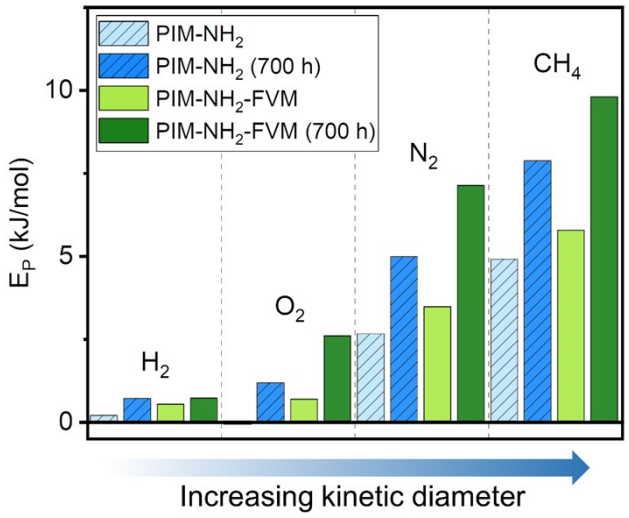

Figure S12. Comparison of activation energy of permeation for fresh and aged PIM-NH_2 and PIM-NH_2-FVM films. The lighter colors indicate fresh samples, and the darker colors indicate aged samples (710 h).

Table S11. Gas permeability and ideal selectivity of tested gases for the variable-temperature study.

Polymer	Aging time[a] (h)	Temp (°C)	Permeability (barrer)				Average selectivity	
			H_2	O_2	N_2	CH_4	H_2/CH_4	O_2/N_2
PIM-NH$_2$	33	35	2520 ± 70	750 ± 20	210 ± 10	290 ± 10	8.7 ± 0.3	3.6 ± 0.1
		45	2510 ± 70	750 ± 20	230 ± 10	330 ± 10	7.5 ± 0.3	3.2 ± 0.1
		55	2530 ± 70	750 ± 20	250 ± 10	390 ± 10	6.6 ± 0.2	3.0 ± 0.1
		65	2550 ± 70	750 ± 20	260 ± 10	430 ± 10	6.0 ± 0.2	2.9 ± 0.1
	710	35	2290 ± 60	590 ± 20	140 ± 10	170 ± 10	13.9 ± 0.5	4.1 ± 0.2
		45	2330 ± 60	620 ± 20	170 ± 10	210 ± 10	11.3 ± 0.4	3.7 ± 0.1
		55	2380 ± 70	630 ± 20	190 ± 10	250 ± 10	9.4 ± 0.4	3.4 ± 0.1
		65	2410 ± 70	640 ± 20	210 ± 10	310 ± 10	7.8 ± 0.3	3.1 ± 0.1
PIM-NH$_2$-FVM	20	35	3200 ± 60	890 ± 20	250 ± 20	320 ± 10	10.0 ± 0.3	3.6 ± 0.1
		45	3240 ± 60	950 ± 20	280 ± 10	380 ± 10	8.6 ± 0.2	3.4 ± 0.1
		55	3270 ± 60	950 ± 20	310 ± 10	440 ± 10	7.4 ± 0.2	3.1 ± 0.1
		65	3340 ± 60	940 ± 20	330 ± 10	500 ± 10	6.6 ± 0.2	2.9 ± 0.1
	710	35	2910 ± 60	610 ± 10	120 ± 10	130 ± 10	22.7 ± 0.6	4.9 ± 0.1
		45	2960 ± 60	660 ± 10	150 ± 10	170 ± 10	17.5 ± 0.5	4.3 ± 0.1
		55	3020 ± 60	710 ± 10	190 ± 10	220 ± 10	13.7 ± 0.4	3.8 ± 0.1
		65	3070 ± 60	750 ± 10	220 ± 10	280 ± 10	11.0 ± 0.3	3.4 ± 0.1

[a]The presented time is the aging time at the start of hydrogen permeation test. All tests were completed within 4 hours unless indicated otherwise.

Table S12. Activation energy of permeation of H_2, O_2, N_2, and CH_4 for the polymers studied in this work.

Polymer	Aging time[a] (h)	Activation energy of permeation (kJ mol^{-1})			
		H_2	O_2	N_2	CH_4
PIM-NH$_2$	33	0.166	−0.095	2.632	4.883
	710	0.678	1.152	4.959	7.853
PIM-NH$_2$-FVM	20	0.508	0.657	3.450	5.761
	710	0.690	2.575	7.111	9.791

[a]The presented time is the aging time at the start of hydrogen permeation test. All tests were completed within 4 hours unless indicated otherwise.

7. Fractional free volume (FFV) dependence on permeability changes on a normalized scale

Permeability (P) and fractional free volume (FFV) are typically correlated by the following equation:[19]

$$P = Ae^{-\frac{B}{FFV}} \#(S1)$$

where A and B are gas-specific constants. By using this correlation, we can derive an equation for the normalized permeability as follows:

$$\frac{P}{P_0} = \exp\left(\frac{B}{FFV_0} - \frac{B}{FFV}\right) \#(S2)$$

where FFV_0 is the initial fractional free volume and FFV is the fractional free volume of an aged sample. By using this relationship between the normalized permeability and FFV_0, we can generate sensitivity plots of how normalized permeability, which is directly related to percent change, is impacted by the initial FFV. **Figure S13** presents examples of these sensitivity plots generated for hydrogen (B = 1.645) and methane gas (B = 2.369).[19] As shown in the figure, the contour lines are slanted, suggesting that initial fractional free volume indeed matters to the amount of decrease observed for normalized permeability. Additionally, we can also observe that the size of gas molecules also affects in these sensitivity plots. For example, consider two polymers with FFV_0 of 0.3 and 0.2. If both polymers' FFV decrease by 0.01 due to physical aging, the normalized permeability of the polymer with FFV_0 = 0.3 will be approximately 0.84 for hydrogen and 0.76 for methane, whereas those for the polymer with FFV_0 = 0.2 will be approximately 0.67 for hydrogen and 0.54 for methane. This suggests that the polymer with lower initial FFV will generally show a larger drop in a normalized scale (e.g., PIM-NH_2 and PIM-NH_2-FVM), and it is

difficult to completely isolate the effect of physical aging factors (e.g., hydrogen bonding and crosslinking) from this effect when comparing different samples with different initial FFV. Thus, physical aging should be studied both in terms of gas transport properties as well as free volume (or packing density). Similar sensitivity plots can be produced for diffusivity since diffusivity is typically correlated by an equation with an identical form to that of *Eq. S1*:[20]

$$D = A^* e^{-\frac{B^*}{FFV}} \#(S3)$$

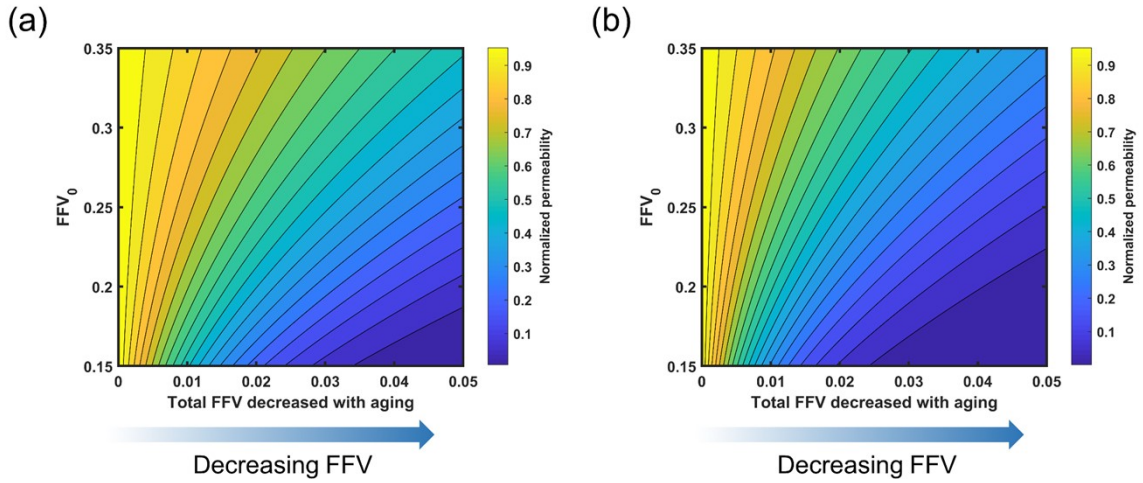

Figure S13. Sensitivity plots of normalized permeability to initial fractional free volume (FFV_0) for (a) hydrogen and (b) methane. Y-axis is the FFV_0, and x-axis is the absolute amount of the fractional free volume decreased with aging.

8. Wide-angle X-ray scattering (WAXS)

Table S13. *d*-spacing calculated from WAXS patterns.

Polymer	Aging time[a] (h)	*d*-spacing (Å)			Changes in *d*-spacing (%)		
		Peak 1	Peak 2	Peak 3	Peak 1	Peak 2	Peak 3
PIM-1	3	6.84	4.96	3.83	−1.53	−1.33	−1.47
	1369	6.73	4.89	3.77			
PIM-NH$_2$	5	6.71	4.91	3.89	−1.27	−1.28	−1.70
	1377	6.62	4.85	3.82			
PIM-NH$_2$-FVM	4	6.67	4.96	3.85	−2.09	−2.49	−1.95
	1369	6.53	4.83	3.78			

[a]The presented time is the aging time at the start of WAXS experiment.

9. Positron anihillation lifetime spectroscopy (PALS)

Table S14. A summary of parameters obtained from PALS, including *o*-Ps lifetimes (τ_3 and τ_4) and intensities (I_3 and I_4). PALS experiments were performed on the samples from our previous study[2] that had been aged for approximately 20,000 h (833 days).

Aging time[a] (h)		**PIM-1** 19,170	**PIM-NH_2** 21,050	**PIM-NH_2-FVM** 19,150
Fresh[b]	τ_3 (ns)	2.4 ± 0.2	2.2 ± 0.1	2.3 ± 0.1
	τ_4 (ns)	7.17 ± 0.05	5.71 ± 0.04	5.7 ± 0.1
	I_3 (%)	5.8 ± 0.2	5.3 ± 0.2	6.3 ± 0.4
	I_4 (%)	17.9 ± 0.3	20.7 ± 0.3	20.2 ± 0.4
Aged	τ_3 (ns)	1.5 ± 0.1	1.7 ± 0.1	1.7 ± 0.1
	τ_4 (ns)	6.59 ± 0.04	5.37 ± 0.03	5.57 ± 0.04
	I_3 (%)	5.8 ± 0.4	5.6 ± 0.2	5.8 ± 0.2
	I_4 (%)	15.1 ± 0.2	22.2 ± 0.3	18.9 ± 0.3

[a]The presented time is the aging time at the start of PALS experiment.
[b]PALS data for fresh samples are from previous study.[2]

10. References

1 S. Thomas, I. Pinnau, N. Du and M. D. Guiver, *J. Membr. Sci.*, 2009, **333**, 125–131.

2 K. Mizrahi Rodriguez, S. Lin, A. X. Wu, G. Han, J. J. Teesdale, C. M. Doherty and Z. P. Smith, *Angew. Chem. Int. Ed.*, 2021, **60**, 6593–6599.

3 R. R. Tiwari, J. Jin, B. D. Freeman and D. R. Paul, *J. Membr. Sci.*, 2017, **537**, 362–371.

4 F. Y. Li and T. S. Chung, *Int. J. Hydrog. Energy*, 2013, **38**, 9786–9793.

5 R. Hou, S. J. D. Smith, C. D. Wood, R. J. Mulder, C. H. Lau, H. Wang and M. R. Hill, *ACS Appl. Mater. Interfaces*, 2019, **11**, 6502–6511.

6 Q. Song, S. Cao, R. H. Pritchard, B. Ghalei, S. A. Al-Muhtaseb, E. M. Terentjev, A. K. Cheetham and E. Sivaniah, *Nat. Commun.*, 2014, **5**, 4813.

7 C. A. Scholes and S. Kanehashi, *Membranes*, 2019, **9**, 41.

8 P. Bernardo, F. Bazzarelli, F. Tasselli, G. Clarizia, C. R. Mason, L. Maynard-Atem, P. M. Budd, M. Lanč, K. Pilnáček, O. Vopička, K. Friess, D. Fritsch, Y. P. Yampolskii, V. Shantarovich and J. C. Jansen, *Polymer*, 2017, **113**, 283–294.

9 X. Wu, Y. Ren, G. Sui, G. Wang, G. Xu, L. Yang, Y. Wu, G. He, N. Nasir, H. Wu and Z. Jiang, *AIChE J.*, 2020, **66**, e16800.

10 W. F. Yong, F. Y. Li, Y. C. Xiao, P. Li, K. P. Pramoda, Y. W. Tong and T. S. Chung, *J. Membr. Sci.*, 2012, **407**–**408**, 47–57.

11 L. Hao, P. Li and T. S. Chung, *J. Membr. Sci.*, 2014, **453**, 614–623.

12 X. M. Wu, Q. G. Zhang, P. J. Lin, Y. Qu, A. M. Zhu and Q. L. Liu, *J. Membr. Sci.*, 2015, **493**, 147–155.

13 C. Z. Liang, J. T. Liu, J. Y. Lai and T. S. Chung, *J. Membr. Sci.*, 2018, **563**, 93–106.

14 X. Chen, Z. Zhang, L. Wu, X. Liu, S. Xu, J. E. Efome, X. Zhang and N. Li, *ACS Appl. Polym. Mater.*, 2020, **2**, 987–995.

15 N. Du, G. P. Robertson, I. Pinnau and M. D. Guiver, *Macromolecules*, 2010, **43**, 8580–8587.

16 N. Du, G. P. Robertson, J. Song, I. Pinnau, S. Thomas and M. D. Guiver, *Macromolecules*, 2008, **41**, 9656–9662.

17 Z. G. Wang, X. Liu, D. Wang and J. Jin, *Polym. Chem.*, 2014, **5**, 2793–2800.

18 M. M. Khan, S. Shishatskiy and V. Filiz, *Membranes*, 2018, **8**, 1.

19 A. X. Wu, S. Lin, K. Mizrahi Rodriguez, F. M. Benedetti, T. Joo, A. F. Grosz, K. R. Storme, N. Roy, D. Syar and Z. P. Smith, *J. Membr. Sci.*, 2021, **636**, 119526.

20 D. F. Sanders, Z. P. Smith, R. Guo, L. M. Robeson, J. E. McGrath, D. R. Paul and B. D.

Freeman, *Polymer*, 2013, **54**, 4729–4761.